Inorg. Chem. **2007**, *46*, 5059–5068

Dual Triggering of DNA Binding and Fluorescence via Photoactivation of a Dinuclear Ruthenium(II) Arene Complex

Steven W. Magennis,*,† Abraha Habtemariam,‡ Olga Novakova,§ John B. Henry,‡ Samuel Meier,‡ Simon Parsons,‡ Iain D. H. Oswald,‡ Viktor Brabec,§ and Peter J. Sadler*,‡

School of Physics and the Collaborative Optical Spectroscopy, Micromanipulation and Imaging Centre (COSMIC), The University of Edinburgh, King's Buildings, Edinburgh EH9 3JZ, U.K., School of Chemistry, The University of Edinburgh, King's Buildings, Edinburgh EH9 3JJ, U.K., and Institute of Biophysics, Academy of Sciences of the Czech Republic, v.i.i. Kralovopolska 135, CZ-61265 Brno, Czech Republic

Received November 6, 2006

The dinuclear Ru^{II} arene complexes $[\{(\eta^6\text{-arene})RuCl\}_2(\mu\text{-2,3-dpp})](PF_6)_2$, arene = indan (**1**), benzene (**2**), *p*-cymene (**3**), or hexamethylbenzene (**4**) and 2,3-dpp = 2,3-bis(2-pyridyl)pyrazine, have been synthesized and characterized. Upon irradiation with UVA light, complexes **1** and **2** readily underwent arene loss, while complexes **3** and **4** did not. The photochemistry of **1** was studied in detail. In the X-ray structure of $[\{(\eta^6\text{-indan})RuCl\}_2(\mu\text{-2,3-dpp})](PF_6)_2$ (**1**), 2,3-dpp bridges two Ru^{II} centers 6.8529(6) Å apart. In water, aquation of **1** in the dark occurs with replacement of chloride with biexponential kinetics and decay constants of 100 ± 1 min^{-1} and 580 ± 11 min^{-1}. This aquation was suppressed by 0.1 M NaCl. UV or visible irradiation of **1** in aqueous or methanolic solution led to arene loss. The fluorescence of the unbound arene is ~40 times greater than when it is complexed. Irradiation of **1** also had a significant effect on its interactions with DNA. The DNA binding of **1** is increased after irradiation. The non-irradiated form of **1** preferentially formed DNA adducts that only weakly blocked RNA polymerase, while irradiation of **1** transformed the adducts into stronger blocks for RNA polymerase. The efficiency of irradiated **1** to form DNA interstrand cross-links was slightly greater than that of cisplatin in both 10 mM $NaClO_4$ and 0.1 M NaCl. In contrast, the interstrand cross-linking efficiency of non-irradiated **1** in 10 mM $NaClO_4$ was relatively low. An intermediate amount of cross-linking was observed when the sample of DNA already modified by non-irradiated **1** was irradiated. DNA unwinding measurements supported the conclusion that both mono- and bifunctional adducts with DNA can form. These results show that photoactivation of dinuclear Ru^{II} arene complexes can simultaneously produce a highly reactive ruthenium species that can bind to DNA and a fluorescent marker (the free arene). Importantly, the mechanism of photoreactivity is also independent of oxygen. These complexes, therefore, have the potential to combine both photoinduced cell death and fluorescence imaging of the location and efficiency of the photoactivation process.

Introduction

Anticancer treatments that use site-selective photoinduced cytotoxicity have the potential to eliminate the unwanted side effects of conventional chemotherapy by avoiding damage to healthy cells. Photoactivation may also allow new and more toxic reaction pathways to be accessed. Photodynamic therapy (PDT), which involves the use of drugs (usually porphyrins or related molecules) that absorb light and subsequently react with cellular components to produce cytotoxic species, has received the most attention to date.[1] The most widely used drug, Photofrin, is an ill-defined mixture of up to 60 different substances and remains in the body for six to eight weeks, resulting in prolonged skin sensitivity. Photofrin requires oxygen for its mechanism of toxicity in PDT, even though tumors often have poor oxygen

* To whom correspondence should be addressed. E-mail: s.magennis@ed.ac.uk (S.W.M.); p.j.sadler@ed.ac.uk (P.J.S.).
† School of Physics and Collaborative Optical Spectroscopy, Micromanipulation and Imaging Centre (COSMIC), The University of Edinburgh.
‡ School of Chemistry, The University of Edinburgh.
§ Institute of Biophysics, Academy of Sciences of the Czech Republic.

(1) Dolmans, D. E. J. G. J.; Fukumura, D.; Jain, R. K. *Nat. Rev. Cancer* **2003**, *3*, 380−387.

10.1021/ic062111q CCC: $37.00
Published on Web 05/12/2007

supply. Second-generation photosensitizers address some of these problems, but despite progress, PDT is not yet considered to be a front-line treatment for cancer. Therefore, there is a need for alternative photoactive drugs.

The unique reactivity of metal complexes makes them interesting candidates for chemotherapy.[2] A notable example is the platinum drug cisplatin, *cis*-$[Pt^{II}(NH_3)_2Cl_2]$, one of the most widely used anticancer agents for chemotherapy, despite its severe side-effects and acquired drug resistance.[2] This drug and several other platinum anticancer complexes are believed to act through formation of adducts with cellular DNA. In principle, metal-based photoactivated anticancer drugs might offer significant advantages over porphyrin-based phototherapies. Much progress has been made in this area over the past decade.[3,4] Metallointercalators can photocleave nucleic acids from DNA,[5] photoreactions of Pt^{IV} azide complexes can induce Pt^{II}−DNA cross-links similar to those established for cisplatin,[6,7] while the photochemistry of many other metal complexes has also been studied.[8−15]

The present study concerns a ruthenium complex in the class [(η^6-arene)Ru(XY)Z], where XY is a chelating diamine and Z is a leaving group such as Cl^-. Such "piano-stool" complexes have been shown to be cytotoxic to cancer cell lines, including lines that have become resistant to cisplatin.[16] Furthermore, previous studies with platinum compounds have shown that dinuclear complexes can lead to novel DNA lesions, which can be important in the avoidance of cellular cross-resistance.[17] Here we report the synthesis, characterization, and photochemistry of organometallic dinuclear Ru^{II} complexes [{(η^6-arene)RuCl}$_2$(μ-2,3-dpp)]$(PF_6)_2$ containing 2,3-dpp (2,3-bis(2-pyridyl)pyrazine) as a bridging ligand and

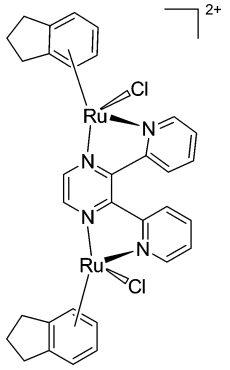

Figure 1. Structure of [{(η^6-indan)RuCl}$_2$(μ-2,3-dpp)]$(PF_6)_2$ (**1**).

Scheme 1. Thermal and Photoreactivity of **1**

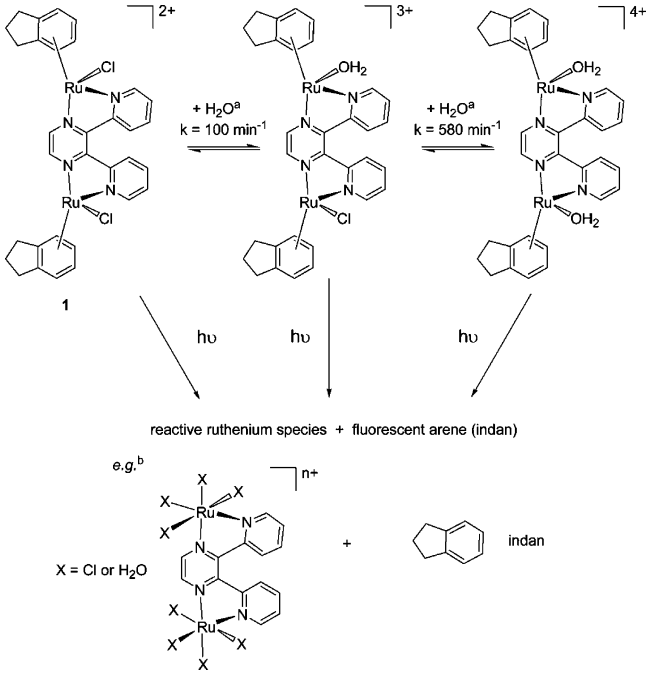

[a] Note that additional hydroxo complexes may also exist because of the deprotonation of aqua ligands. [b]The ruthenium species indicated here are only possible photoproducts. The detailed photochemical reaction pathways will be the subject of further investigation.

indan (**1**), benzene (**2**), *p*-cymene (**3**), or hexamethylbenzene (**4**) as the arene. We show that [{(η^6-indan)RuCl}$_2$(μ-2,3-dpp)]$(PF_6)_2$ (**1**), Figure 1, can be photoactivated to produce a highly reactive ruthenium species that can bind to DNA and a fluorescent marker (Scheme 1). Importantly, the mechanism of photoreactivity is also independent of oxygen. These complexes, therefore, have the potential to combine both photoinduced cell death and fluorescence imaging of the location and efficiency of the photoactivation process.

Experimental Section

Materials. $[Ru(bpy)_3)]Cl_2 \cdot 6H_2O$ (bpy = 2,2′-bipyridine) (99.5%), 2,3-bis(2-pyridyl)-pyrazine (2,3-dpp), indan (95%), and NH_4PF_6 were obtained from Aldrich. Cisplatin was obtained from Sigma. $[Ru(indan)Cl_2]_2$ was prepared following literature methods.[18] NaCl (reagent grade) was obtained from Fisher. The solvents used for photochemistry and fluorescence spectroscopy were methanol and

(2) Guo, Z. J.; Sadler, P. J. *Angew. Chem., Int. Ed.* **1999**, *38*, 1513−1531.
(3) Clarke, M. J. *Coord. Chem. Rev.* **2003**, *236*, 209−233.
(4) Szaciłwski, K.; Macyk, W.; Drzewiecka-Matuszek, A.; Brindell, M.; Stochel, G. *Chem. Rev.* **2005**, *105*, 2647−2694.
(5) Erkkila, K. E.; Odom, D. T.; Barton, J. K. *Chem. Rev.* **1999**, *99*, 2777−2795.
(6) Müller, P.; Schröder, B.; Parkinson, J. A.; Kratochwil, N. A.; Coxall, R. A.; Parkin, A.; Parsons, S.; Sadler, P. J. *Angew. Chem., Int. Ed.* **2003**, *42*, 335−339.
(7) Kratochwil, N. A.; Parkinson, J. A.; Bednarski, P. J.; Sadler, P. J. *Angew. Chem., Int. Ed.* **1999**, *38*, 1460−1463.
(8) Brindell, M.; Kuliś, E.; Elmroth, S. K. C.; Urbańska, K.; Stochel, G. *J. Med. Chem.* **2005**, *48*, 7298−7304.
(9) Holder, A. A.; Swavey, S.; Brewer, K. J. *Inorg. Chem.* **2004**, *43*, 303−308.
(10) Benites, P. J.; Holmberg, R. C.; Rawat, D. S.; Kraft, B. J.; Klein, L. J.; Peters, D. G.; Thorp, H. H.; Zaleski, J. M. *J. Am. Chem. Soc.* **2003**, *125*, 6434−6446.
(11) Singh, T. N.; Turro, C. *Inorg. Chem.* **2004**, *43*, 7260−7262.
(12) Lutterman, D. A.; Fu, P. K.-L.; Turro, C. *J. Am. Chem. Soc.* **2006**, *128*, 738−739.
(13) Menon, E. L.; Perera, R.; Navarro, M.; Kuhn, R. J.; Morrison, H. *Inorg. Chem.* **2004**, *43*, 5373−5381.
(14) Uji-i, H.; Foubert, P.; De Schryver, F. C.; De Feyter, S.; Gicquel, E.; Etoc, A.; Moucheron, C.; Kirsch-De Mesmaeker, A. *Chem. Eur. J.* **2006**, *12*, 758−762.
(15) Gicquel, E.; Paillous, N.; Vicendo, P. *Photochem. Photobiol.* **2000**, *72*, 583−589.
(16) Aird, R. E.; Cummings, J.; Ritchie, A. A.; Muir, M.; Morris, R. E.; Chen, H.; Sadler, P. J.; Jodrell, D. I. *Br. J. Cancer* **2002**, *86*, 1652−1657.
(17) Zaludova, R.; Zakovska, A.; Kasparkova, J.; Balcarova, Z.; Kleinwachter, V.; Vrana, O.; Farrell, N.; Brabec, V. *Eur. J. Biochem.* **1997**, *246*, 508−517.
(18) Bennett, M. A.; Smith, A. K. *J. Chem. Soc., Dalton Trans.* **1974**, 233−241.

water (HPLC, Fisher). NMR spectroscopy used methanol-d_4 (99.8%), acetonitrile-d_3, and D_2O from Aldrich.

Preparation and Characterization of [{(η^6-Indan)RuCl}$_2$(μ-2,3-dpp)](PF$_6$)$_2$ (1). The dimer [Ru(indan)Cl$_2$]$_2$ (0.150 g, 0.26 mmol) was dissolved in MeOH (40 mL), and 2,3-dpp (0.077 g, 0.30 mmol) was added to this mixture. The solution turned deep red, and the reaction mixture was stirred at ambient temperature for 1.5 h. It was then filtered, and the volume of the filtrate was reduced on a rotary evaporator to ~25 mL. NH_4PF_6 (0.254 g, 1.56 mmol) was added to the mixture, and the flask was shaken. A precipitate started to appear almost immediately. The flask was kept at 253 K overnight. The precipitate was collected by filtration, washed with cold methanol and ether, and dried in air to give an orange-red solid (yield: 200 mg, 75%). Crystals suitable for X-ray diffraction studies were obtained by slow evaporation of a methanolic solution at ambient temperature. ^{1}H NMR (CD_3CN-d_3): δ 9.20 (d, 2H), 9.17 (m, 2H) 8.45 (d, 2H), 8.02 (t, 2H), 7.79 (t, 2H), 6.10−5.86 (m, 8H), 3.09−2.78 (m, 8H), 2.18 (m, 4H). Anal. Calcd for $C_{32}H_{30}Cl_2F_{12}N_4P_2Ru_2$: C, 37.19; H, 2.93; N, 5.42. Found: C, 36.9; H, 3.68; N, 5.58.

The three other dinuclear ruthenium(II) arene complexes in the series [{(η^6-arene)RuCl}$_2$(μ-2,3-dpp)](PF$_6$)$_2$, where arene = benzene (**2**), *p*-cymene (**3**), or hexamethylbenzene (**4**), were synthesized and characterized as described in the Supporting Information.

NMR Spectroscopy. ^{1}H NMR spectra were acquired on a Bruker DMX 500 spectrometer (^{1}H = 500 MHz). All data processing was carried out using XWIN NMR, version 2.0 (Bruker U.K. Ltd.). ^{1}H NMR chemical shifts for aqueous solutions were internally referenced to 1,4-dioxane (3.77 ppm), to the methyl singlet of TSP (0 ppm), or to residual protiated solvent in acetonitrile-d_3 (1.94 ppm) and methanol-d_4 (3.31 ppm).

X-ray Crystallography. Diffraction data were collected using Mo Kα radiation (λ = 0.71073 Å) on a Bruker Smart Apex CCD diffractometer equipped with an Oxford Cryosystems LT device operating at 150 K. Crystals suitable for X-ray diffraction were grown from a methanol solution at ambient temperature: orange block of dimensions 0.12 × 0.12 × 0.12 mm^3; formula $C_{33}H_{34}Cl_2F_{12}N_4OP_2Ru_2$, M = 1065.62; monoclinic, space group $P2_1/n$; a = 12.1038(8) Å, b = 16.8908(11) Å, c = 18.8556(12) Å, β = 101.1960(10)°, V = 3781.5(4) Å^3; Z = 4, D_{calcd} = 1.872 Mg m^{-3}; μ = 1.120 mm^{-1}; $F(000)$ = 2112. The structure was solved using direct methods (SHELXS)[19] and was refined against F^2 using SHELXL.[20] Hydrogen atoms were placed in calculated positions, and the non-H atoms were refined with anisotropic displacement parameters. The final conventional R factor [R1, based on $|F|$ and 6645 data points with $F > 4\sigma(F)$] was 0.0381, and the weighted wR2 (based on F^2 and all 7741 unique data from θ = 1.6 to 26.4°) was 0.0810. The final ΔF synthesis extremes were +0.77 and −0.51 e Å^{-3}.

Photochemistry and Fluorescence Spectroscopy. UV−vis spectra were recorded on a Cary 50-Bio spectrophotometer. Typical concentrations of **1** were 0.05−0.2 mM. Solutions were stored in the dark to minimize unwanted photoreactions between measurements. For photochemical studies, methanolic or aqueous solutions of **1** were irradiated with a high-pressure mercury lamp (Nikon model LH-M100CB-1). The lamp output was passed through a bandpass filter (Nikon) in the range of 340−380 or 465−495 nm and was focused onto the sample cuvette, providing average light power of 100 and 42 mW, respectively. Solutions were handled in air at room temperature (~294 K), unless stated otherwise. The effect of oxygen on the photochemistry was assessed by degassing methanolic solutions using three freeze−pump−thaw cycles to a final pressure of 6.4−7.4 mbar for 5 min. Care was taken to minimize the exposure of the degassing cell to light during the degassing procedure, with spectra recorded before and after degassing to ensure that no reaction had taken place during the process. The degassing procedure was verified by observation of the reversible increase in fluorescence of [Ru(bpy)$_3$]Cl$_2$ in methanol upon degassing.[21]

Time-resolved fluorescence measurements were made by time-correlated single-photon counting (TCSPC). The output of a femtosecond laser system (10 W Verdi and Mira Ti-Sapphire laser, Coherent) was passed through a pulse picker (to reduce the repetition rate to 4.75 MHz) and frequency tripled to either 260 nm for **1** or to 300 nm for [Ru(bpy)$_3$]Cl$_2$ and biphenyl. The fluorescence was measured at the magic angle in a spectrometer equipped with TCC900 photon-counting electronics (Edinburgh Instruments). The emission monochromator bandpass was 9 nm. The instrument response was ~50 ps full width at half-maximum. Decay curves were analyzed with tail fits using F900 software (Edinburgh Instruments). The quality of these fits was determined by the value of the χ^2 statistical parameter and visualization of residuals. Steady-state fluorescence spectra were either acquired using a SPEX Fluoromax (λ_{ex} = 260 nm; 5 nm excitation and emission slits) or with the same setup used for time-resolved measurements above. There was negligible solvent fluorescence.

The photochemical quantum yield of **1** in 0.1 M NaCl with excitation through the 340−380 nm filter was estimated by measurement of the lamp power at 360 nm with a calibrated power meter (Fieldmaster with LM10 head, Coherent) and the absorption of the complex at the excitation wavelength. It was assumed that the photochemical reaction had gone to completion when there was no further change in absorption or fluorescence. The photochemical quantum yield was measured by calculation of the amount of light required to convert 20% of the sample to product. No corrections were made for absorption by the photoproducts or reflection of the excitation light from the surfaces of the cuvette.

Kinetic parameters for aquation of **1** were obtained by fitting the curve of absorbance of **1** in water at 440 nm versus time to a biexponential decay (linear least-squares fitting in Origin 7 software).

DNA Binding. Reaction mixtures of DNA and **1** were prepared in three ways: in the dark (henceforth referred to as "non-irradiated"), by addition of pre-irradiated **1** to DNA ("pre-irradiated"), or by addition of **1** to DNA followed by irradiation of the resulting mixture ("irradiated"). A stock solution of **1** at a concentration of 5 × 10^{-4} M in 10 mM $NaClO_4$ was prepared in the dark at 298 K. A sample of **1** dissolved in 0.1 M NaCl was prepared by the addition of NaCl to a stock solution of **1** in 10 mM $NaClO_4$. Pre-irradiated samples of **1** were prepared by irradiation of the stock solution of **1** in 10 mM $NaClO_4$. Calf thymus (CT) DNA (42% G + C, mean molecular mass ~20 000 kD) was prepared and characterized as described previously.[22,23] Plasmid pSP73KB [2455 base pairs (bp)] was isolated according to standard procedures. Restriction endonucleases and Klenow fragment of DNA polymerase I were purchased from New England Biolabs. Riboprobe Gemini System II for transcription mapping containing T7 RNA polymerase was purchased from Promega and ethidium

(19) Sheldrick, G. M. *SHELXS*; University of Göttingen: Göttingen, Germany, 1997.
(20) Sheldrick, G. M. *SHELXL*; University of Göttingen: Göttingen, Germany, 1997.
(21) Demas, J. N.; McBride, R. P.; Harris, E. W. *J. Phys. Chem.* **1976**, *80*, 2248−2253.
(22) Brabec, V.; Palecek, E. *Biophysik* **1970**, *6*, 290−300.
(23) Brabec, V.; Palecek, E. *Biophys. Chem.* **1976**, *4*, 79−92.

bromide and agarose from Merck KgaA (Darmstadt, Germany). Acrylamide, bis(acrylamide), and urea were purchased from Merck KgaA, and the radioactive products were obtained from MP Biomedicals, LLC (Irvine, CA).

Irradiation. Samples were irradiated at 310 K using the LZC-4V illuminator (photoreactor) (Luzchem, Canada) with temperature controller and with UVA lamps (300−400 nm with a maximum intensity at ∼360 nm, 5 mW cm^{-2}) for 60 min.

Ruthenation Reactions. CT DNA and plasmid pSP73KB were incubated with **1** in 10 mM $NaClO_4$ or 0.1 M NaCl at 310 K. The number of atoms of ruthenium bound per nucleotide residue (r_b value) was determined by flameless atomic absorption spectrophotometry (FAAS).

DNA Transcription by RNA Polymerase In Vitro. Transcription of the (*Nde*I/*Hpa*I) restriction fragment of pSP73KB DNA with DNA-dependent T7 RNA polymerase and electrophoretic analysis of transcripts were performed according to the protocols recommended by Promega [Promega Protocols and Applications, 43−46 (1989/90)] and were previously described in detail.[24,25]

DNA Interstrand Cross-linking. The amount of interstrand cross-links formed by **1** in linear DNA was measured in pSP73KB plasmid (2455 bp), which was first linearized by *Eco*RI (*Eco*RI cuts only once within pSP73 plasmid), 3′-end labeled by means of Klenow fragment of DNA polymerase I in the presence of [α-^{32}P]-dATP, and subsequently modified by the ruthenium complex. Linearized DNA (1 μg) was incubated with the complex for 20 h so that an r_b value of 0.001 was reached, unless stated otherwise. The samples were precipitated by ethanol to remove unbound ruthenium, and the pellet was dissolved in 18 μL of a solution containing 30 mM NaOH, 1 mM EDTA, 6.6% sucrose, and 0.04% bromophenol blue. The samples were analyzed for interstrand CLs by agarose gel electrophoresis under denaturing conditions (on alkaline 1% agarose gel).[25,26] After the electrophoresis was completed, the intensities of the bands corresponding to single strands of DNA and interstrand cross-linked duplex were quantified by means of a Phosphor Imager (Fuji BAS 2500 system with AIDA software). The frequency of the interstrand cross-links (the number of interstrand cross-links per molecule of the ruthenium complex bound to DNA) was calculated using the Poisson distribution from the fraction of non-cross-linked DNA in combination with the r_b values and the fragment size. Other details of this assay can be found in previously published papers.[25−27]

Unwinding of Negatively Supercoiled DNA. The unwinding of closed circular supercoiled pSP73KB plasmid DNA was assayed by an agarose gel mobility shift assay.[28] The unwinding angle, Φ, induced per DNA adduct of **1** was calculated upon the determination of the r_b value at which the complete transformation of the supercoiled to relaxed form of the plasmid was attained. Samples of the pSP73KB plasmid were incubated with **1** for 20 h, precipitated by ethanol, and redissolved in TAE buffer (0.04 M Tris-acetate + 1 mM EDTA, pH 7.0). An aliquot of the precipitated sample was subjected to electrophoresis on 1% agarose gels running at 298 K in the dark with TAE buffer at 30 V. The gels were then stained with ethidium bromide, followed by photography on Polaroid 667 film with transilluminator. The other aliquot was used for the determination of the r_b values by FAAS.

Table 1. Selected Bond Lengths (Å) and Angles (deg) for **1**[a]

Ru(1A)−Cl(1A)	2.3853(9)
Ru(1B)−Cl(1B)	2.3947(8)
Ru(1A)−N1	2.082(3)
Ru(1A)−N8	2.075(3)
Ru(1B)−N11	2.057(3)
Ru(1B)−N18	2.074(3)
Ru(1A)−C(1A)	2.184(4)
Ru(1A)−C(2A)	2.213(3)
Ru(1A)−C(6A)	2.222(3)
Ru(1A)−C(7A)	2.201(4)
Ru(1A)−C(8A)	2.149(4)
Ru(1A)−C(9A)	2.182(4)
Ru(1B)−C(1B)	2.194(3)
Ru(1B)−C(2B)	2.205(3)
Ru(1B)−C(6B)	2.221(9)
Ru(1B)−C(7B)	2.188(3)
Ru(1B)−C(8B)	2.182(3)
Ru(1B)−C(9B)	2.165(3)
N1−Ru(1A)−N8	76.75(10)
N11−Ru(1B)−N18	76.64(10)

[a] For the numbering scheme, see Figure 2.

Other Methods. FAAS measurements were made on a Varian AA240Z Zeeman atomic absorption spectrometer equipped with a GTA 120 graphite tube atomizer. The gels were dried and visualized by using the FUJIFILM bioimaging analyzer, and the radioactivities associated with bands were quantified with AIDA image analyzer software.

Results and Discussion

Synthesis and Characterization. The bimetallic complexes [{(η^6-arene)RuCl}$_2$(μ-2,3-dpp)](PF$_6$)$_2$, arene = indan (**1**), benzene (**2**), *p*-cymene (**3**), or hexamethylbenzene (**4**), were prepared by the reaction of the appropriate dimer [(η^6-arene)RuCl$_2$]$_2$ with an equimolar amount of 2,3-dpp. The products were isolated as hexafluorophosphate salts and were characterized by ^{1}H NMR spectroscopy, elemental analysis, and for **1**, X-ray crystallography. It is possible that two isomers can form because the coordinated chloride ligands take either cis or trans positions. However, ^{1}H NMR spectroscopy studies suggested that only one species is present in solution, and the solid-state structure of **1** shows that the compound crystallized with the chloride ligands in a cis position (vide infra).

X-ray Crystallography. Crystals of **1** suitable for X-ray diffraction studies were obtained from methanol at 273 K. Selected bond lengths and angles are shown in Table 1, and the structure with numbering scheme is shown in Figure 2. The 2,3-dpp bridge holds the two ruthenium centers at an intermolecular distance of 6.8529(6) Å, which is comparable to those found for other pyrazine-bridged ruthenium dimers (6.779−7.026 Å) (CSD). The Ru−Cl bonds are in a mutually cis configuration with a separation of 6.306(3) Å between chlorides. In contrast, the related bimetallic complex [{(η^6-*p*-cymene)RuCl}$_2$(μ-2,3-dpp)](PF$_6$)$_2$ crystallized with Ru−Cl in a trans configuration.[29] As a consequence, there are major differences in the crystal packing of the two structures.

(24) Lemaire, M. A.; Schwartz, A.; Rahmouni, A. R.; Leng, M. *Proc. Natl. Acad. Sci. U.S.A.* **1991**, *88*, 1982−1985.
(25) Brabec, V.; Leng, M. *Proc. Natl. Acad. Sci. U.S.A.* **1993**, *90*, 5345−5349.
(26) Farrell, N.; Qu, Y.; Feng, L.; Van Houten, B. *Biochemistry* **1990**, *29*, 9522−9531.
(27) Brabec, V.; Kasparkova, J.; Vrana, O.; Novakova, O.; Cox, J. W.; Qu, Y.; Farrell, N. *Biochemistry* **1999**, *38*, 6781−6790.
(28) Keck, M. V.; Lippard, S. J. *J. Am. Chem. Soc.* **1992**, *114*, 3386−3390.
(29) Singh, A.; Singh, S. K.; Trivedi, M.; Pandey, D. S. *J. Organomet. Chem.* **2005**, *690*, 4243−4251.

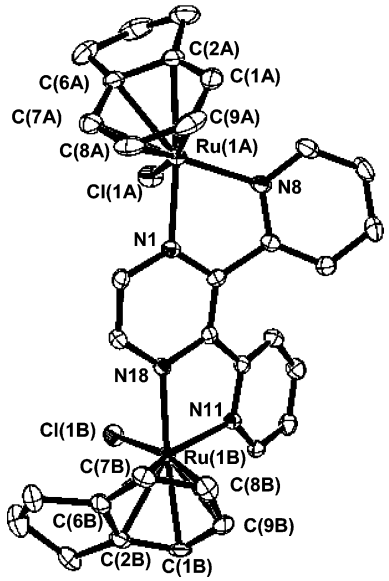

Figure 2. X-ray crystal structure of [{(η^6-indan)RuCl}$_2$(μ-2,3-dpp)](PF$_6$)$_2$ (**1**), showing numbering scheme. Ellipsoids enclose 30% probability surfaces. Ru(1A)−Ru(1B) = 6.8529(6) Å.

Interactions (intra- and inter-) between C−H and X (X = Cl, F), as well as $\pi-\pi$ interactions, in [{(η^6-*p*-cymene)-RuCl}$_2$(μ-2,3-dpp)](PF$_6$)$_2$ are believed to stabilize the crystal packing arrangement, which involves parallel helical chains.[29] This type of packing was not observed in the crystal structure of **1**, where only weak interactions were observed between C−H and F. The bimetallic complexes containing the fragment {Ru^{II}(L)Cl}, L = 2-(C$_5$H$_4$N)−N=N−C$_6$H$_4$Me[30] and L = bipyridine (bpy),[31] bridged by [2,3,5,6-tetrakis(2-pyridyl)pyrazine] (tppz) show both the cis and trans isomers with respect to coordinated chloride ligands in solution, with the former preferentially crystallizing as the trans isomer. Similarly, the bimetallic complex containing two {Ru^{II}([9]-aneS$_3$)Cl} units bridged by 2,2′-bipyrimidine (bpym)[32] show both cis and trans forms with respect to coordinated chloride ligands in solution, with the trans isomer being preferentially crystallized. The Ru−Cl bond lengths for Ru(1A) and Ru-(1B) are slightly different (2.3853 and 2.3947 Å), and the Ru−N distances are in the range of 2.057−2.082 Å. These values are within the range found for other structures of Ru^{II} arene complexes.[33] The 2,3-dpp ligand bridging the two Ru metal centers is substantially distorted from planarity, with the three rings twisting out of plane with respect to one another by 21.74°. The coordination geometry around each ruthenium center is distorted octahedral, which is reflected in the small bite angle of 2,3-dpp [N(1)−Ru(1A)−N(8) (76.75°) and N(11)−Ru(1B)−N(18) (76.64°)], and represents a major deviation from an ideal octahedral geometry; similar distortions were also observed for the bimetallic complexes cited above. The ruthenium-to-arene centroid ring distances [1.6822(15) and 1.6808(14) Å] are slightly longer than those of the Ru^{II} arene complexes containing ethylenediamine (en) but are shorter than those of the Ru^{II} arene complexes containing the π-acidic chelating ligand azopyridine (azpy). For example, the ruthenium-to-arene centroid ring distances for [(η^6-*p*-cymene)RuCl(en)](PF$_6$) and [(η^6-*p*-cymene)RuCl-(azpy)](PF$_6$) are 1.6692(14)[34] and 1.7203(16) Å,[35] respectively. The lengthening of the centroid bond in the latter complex is attributed to an increased extent of back-bonding competition for Ru 4d^6 electron density between the π-acceptor ligands, arene, and azopyridine and may explain the ease of arene loss in solution for this class of complexes.

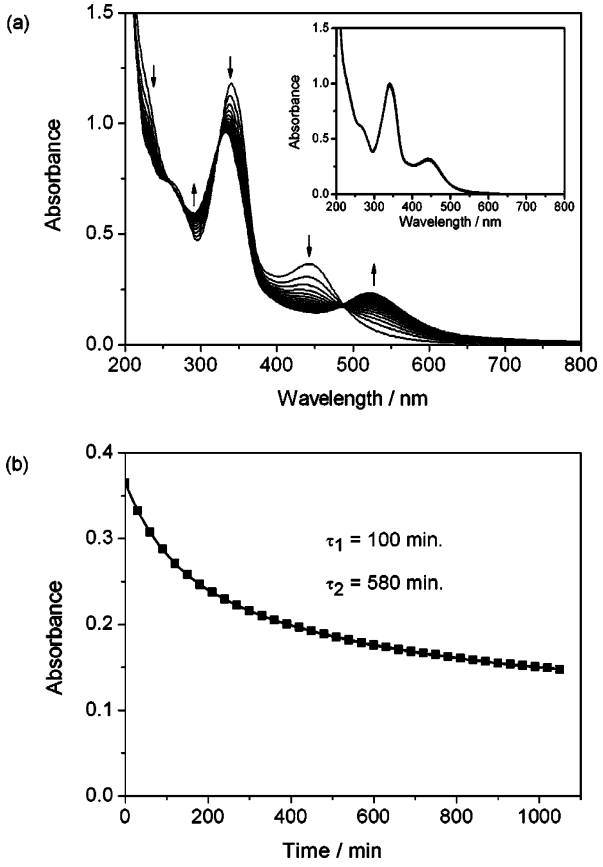

Figure 3. Thermal reactivity of **1** in aqueous solution. (a) Absorption spectra of **1** in water recorded hourly for 17 h. The inset shows the absorption spectra of **1** in 0.1 M NaCl recorded hourly for 18 h. In each case, the first spectrum was recorded ~10 min after dissolution. (b) Time-dependence of absorbance at 440 nm of **1** in water. The solid line is a fit of the data as a biexponential decay, with decay constants of 100 ± 1 and 580 ± 11 min^{-1} and amplitudes of 39 and 61%, respectively (R = 0.9999).

Thermal Reactivity. Freshly dissolved **1** in water undergoes a chemical change in the absence of light. Figure 3a shows absorption spectra recorded every hour for 17 h for a solution of **1** in water. The spectrum immediately after dissolution contains two peaks at 340 ($\epsilon = 1 \times 10^4$ M^{-1}

(30) Chanda, N.; Laye, R. H.; Chakraborty, S.; Paul, R. L.; Jeffery, J. C.; Ward, M. D.; Lahiri, G. K. *J. Chem. Soc., Dalton Trans.* **2002**, 3496−3504.
(31) Hartshorn, C. M.; Daire, N.; Tondreau, V.; Loeb, B.; Meyer, T. J.; White, P. S. *Inorg. Chem.* **1999**, *38*, 3200−3206.
(32) Araújo, C. S.; Drew, M. G. B.; Félix, V.; Jack, L.; Madureira, J.; Newell, M.; Roche, S.; Santos, T. M.; Thomas, J. A.; Yellowlees, L. *Inorg. Chem.* **2002**, *41*, 2250−2259.
(33) Habtemariam, A.; Melchart, M.; Fernández, R.; Parsons, S.; Oswald, I. D. H.; Parkin, A.; Fabbiani, F. P. A.; Davidson, J.; Dawson, A.; Aird, R. E.; Jodrell, D. I.; Sadler, P. J. *J. Med. Chem.* **2006**, *49*, 6858−6868.
(34) Morris, R. E.; Aird, R. E.; Murdoch, P. S.; Chen, H.; Cummings, J.; Hughes, N. D.; Parsons, S.; Parkin, A.; Jodrell, D. I.; Sadler, P. J. *J. Med. Chem.* **2001**, *44*, 3616−3621.
(35) Dougan, S. J.; Melchart, M.; Habtemariam, A.; Parsons, S.; Sadler, P. J. *Inorg. Chem.* **2006**, *45*, 10882−10894.

cm^{-1}) and 440 nm ($\epsilon = 4 \times 10^3\ M^{-1}\ cm^{-1}$). In accordance with the analysis given for related Ru^{II} complexes of bispyridylpyrazine and arenes, the peak at 340 nm is assigned to a LC transition on 2,3-dpp, while the peak at 440 nm is assigned to an MLCT transition from Ru to 2,3-dpp.[36,37] The most apparent change is the decrease in the absorbance of the 440 nm peak and the appearance of a new peak at 520 nm.

The decrease in absorbance at 440 nm with time for **1** in water is shown in Figure 3b. It has a biexponential dependence, as shown by the fit to the data, with decay constants of 100 ± 1 and $580 \pm 11\ min^{-1}$ and amplitudes of 39 and 61%, respectively. Related mononuclear Ru^{II} arene complexes undergo a monoexponential decrease in absorbance because of loss of chloride and substitution by water.[38] In **1**, there are two chloride ligands (one on each Ru) that can be substituted by water. The loss of the first chloride would be expected to be faster than the substitution of the second chloride because of the increased positive charge on the molecule, hence the biexponential kinetics (Scheme 1). This also explains the absence of a clear isosbestic point at around 490 nm in Figure 3a. The new peak at 520 nm in Figure 3a is assigned to an MLCT transition, which is shifted to lower energy for the aqua complex. This is attributed to increased electron density from the water ligand, in comparison to the chloride ligand, which makes the Ru^{II} easier to oxidize.

Experiments were also performed in 0.1 M NaCl. The inset of Figure 3a shows absorption spectra for **1** in 0.1 M NaCl every hour for 18 h. The change in the spectrum with time is negligible, showing that high concentrations of chloride suppress the aquation of **1**.

Photochemistry and Fluorescence Spectroscopy. Ruthenium(II) arene complexes can undergo photoinduced reactions, and this has proven to be a useful synthetic method for the preparation of new ruthenium complexes.[39−41] For example, Ford et al. showed that ruthenium(II) arene complexes of formula $[Ru(\eta^6\text{-arene})L_3]^{2+}$ ($L = NH_3$ or H_2O) undergo loss of the arene and aquation of the metal when irradiated in deaerated aqueous solution.[42] Irradiation of **1** in aqueous or methanolic solutions also resulted in the formation of new species, as evidenced by absorption, NMR, and fluorescence spectroscopy. In general, the course of the photochemical reaction was the same in both water and methanol.

Figure 4 shows the changes in the absorption spectra during irradiation of a 0.1 M NaCl solution of **1**. The new peaks are different from those of the aquated form of **1**. Irradiation of aquated **1** also resulted in spectral changes: the absorption at long wavelength increased, and the peak position shifted from 522 to 530 nm. Furthermore, the photoproducts of **1** in water and 0.1 M NaCl are different (see Figure S1). Similar changes in the absorption spectra were also obtained after irradiation of methanolic solutions of **1** (see Figure S2).

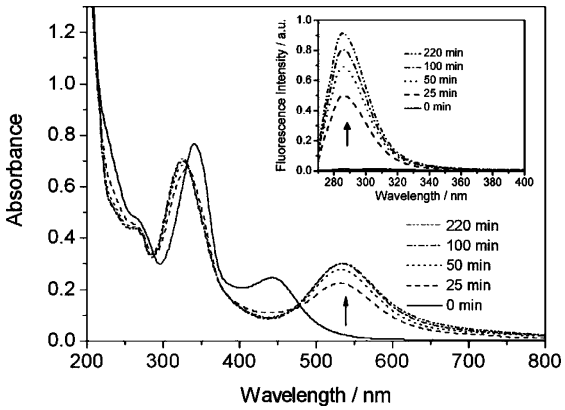

Figure 4. Absorption spectra of **1** in 0.1 M NaCl following irradiation at 340−380 nm (power of 160 mW at 360 nm). Absorption spectra were recorded after 0, 25, 50, 100, and 220 min of irradiation. The inset shows fluorescence spectra for the same solution after irradiation ($\lambda_{ex} = 260$ nm).

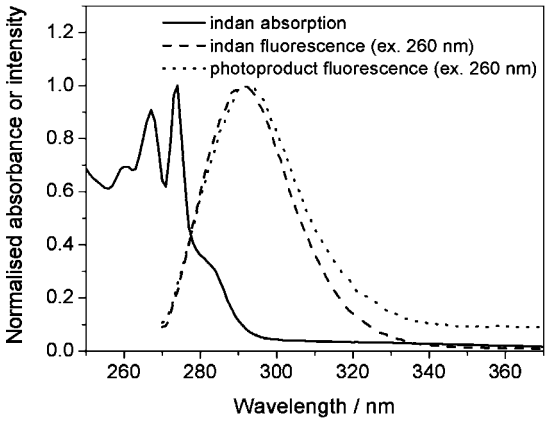

Figure 5. Absorption and fluorescence spectra of indan in methanol and fluorescence spectra of **1** in methanol after irradiation for 220 min ($\lambda_{ex} =$ 260 nm; see Figure S2 for absorption and fluorescence spectra of **1** upon irradiation in methanol).

In addition to the absorption changes, it was found that the solution of **1** became fluorescent as a result of irradiation. Prior to irradiation, **1** was nonemissive when excited in the UV−vis range in water or methanol, with the exception of a weak fluorescence around 285−315 nm when excited at 260-270 nm. After irradiation, this short-wavelength emission increased significantly in intensity (see inset to Figure 4). When excited at 260 nm, the fluorescence in 0.1 M NaCl is ∼40 times greater after irradiation. Since arene loss was a possible explanation for the photochemistry of **1**, the fluorescence of the free arene, indan, was also examined. Figure 5 shows the emission spectrum of the photoproduct of **1** in methanol, together with the absorption and emission spectra for indan in methanol. Indan has a strong absorption in the UV region, with $\epsilon_{267} = 1950\ M^{-1}\ cm^{-1}$ in methanol, and its emission spectrum is very similar to that of the photoproduct. It should be noted that the ligand 2,3-dpp is also emissive when free in solution, but the fluorescence is at a much longer wavelength (peak at 400 nm).

(36) Campagna, S.; Denti, G.; De Rosa, G.; Sabatino, L.; Ciano, M.; Balzani, V. *Inorg. Chem.* **1989**, *28*, 2565−2570.
(37) Di Marco, G.; Bartolotta, A.; Ricevuto, V.; Campagna, S.; Denti, G.; Sabatino, L.; De Rosa, G. *Inorg. Chem.* **1991**, *30*, 270−275.
(38) Wang, F.; Chen, H.; Parsons, S.; Oswald, I. D. H.; Davidson, J. E.; Sadler, P. J. *Chem. Eur. J.* **2003**, *9*, 5810−5820.
(39) Gill, T. P.; Mann, K. R. *Organometallics* **1982**, *1*, 485−488.
(40) Lavallee, R. J.; Kutal, C. *J. Organomet. Chem.* **1998**, *562*, 97−104.
(41) Hayashida, T.; Nagashima, H. *Organometallics* **2002**, *21*, 3884−3888.
(42) Weber, W.; Ford, P. C. *Inorg. Chem.* **1986**, *25*, 1088−1092.

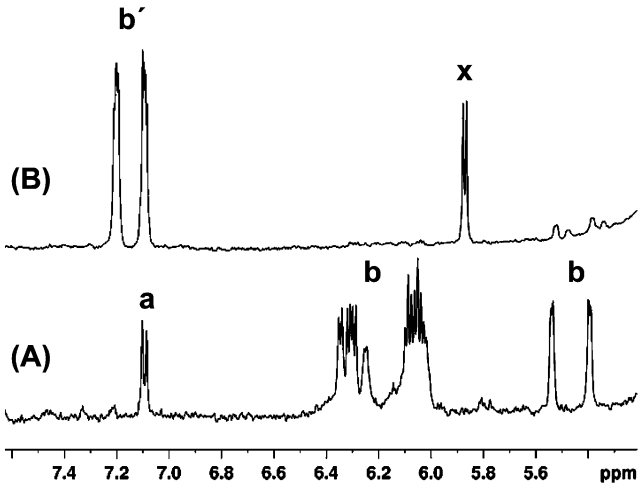

Figure 6. ^{1}H NMR spectra of **1** [{(η^6-indan)RuCl}$_2$(μ-2,3-dpp)](PF$_6$)$_2$ in methanol-d_4 (A) before irradiation, in the dark. Peak assignments: (a) part of bound 2,3-dpp and (b) bound indan. (B) The same sample after irradiation. Peak assignments: (b′) free indan and (x) unassigned. There is also a series of complicated multiplets between 7.5 and 9.8 ppm suggesting that 2,3-dpp is present in a variety of different environments in the products, possibly including polynuclear species.

We used time-resolved fluorescence measurements to help identify the photoproduct. While the fluorescence of indan in methanol fitted a single decay time of 7.96 ns, the photoproduct decay was best described by biexponential kinetics with a major component of 7.97 ns (pre-exponential factor of 92%) and a minor component of 2.06 ns (8%). Therefore, it is clear that irradiation of **1** leads to loss of arene into the solution. The photochemical quantum yield for the reaction of **1** in 0.1 M NaCl was estimated to be $\sim 2 \times 10^{-4}$. The precise nature of the photoproducts is unknown, although plausible species are indicated in Scheme 1. If there is a mixture of photoproducts, then the estimated photochemical quantum yield will represent an average for the different photochemical reactions.

For possible phototherapeutic applications, it is important to assess the importance of oxygen on the photochemistry of **1**. The photolysis of a degassed methanolic solution of **1** was performed under the same conditions that were used for the aerated solutions, and the changes in the absorption spectra were identical to those of the aerated solution. Therefore, oxygen is not involved in the photochemical reaction. It was also necessary to eliminate the possibility of thermal effects during irradiation contributing to the observed spectral changes. The temperature of a solution of **1** in 0.1 M NaCl after irradiation for 25 min (360 nm, 160 mW) was 310−313 K. When an identical solution of **1** was heated in the dark at 328 K for 25 min, this resulted in a small decrease in overall absorption but did not result in the formation of a new band at long wavelength. Therefore, the spectral changes are photoinduced, not thermal.

Confirmation that irradiation of **1** leads to arene loss was provided by ^{1}H NMR spectroscopy. Figure 6 shows ^{1}H NMR spectra of **1** in deuterated methanol before and after irradiation. It is clear that there is a large change in the aromatic region of the ^{1}H spectrum of **1**. In the dark, the peaks at 5.4−5.6 ppm (labeled b) correspond to the protons of indan bound to Ru. After irradiation, new peaks appear at 7.0−7.2 ppm (labeled b′), which have the same chemical shifts as those of free indan. The peaks for 2,3-dpp appear as complicated multiplets after irradiation and were not further analyzed. It is reasonable to suppose that there is a variety of environments for 2,3-dpp in the photoproducts, some of which may be polymeric.

Although only complex **1** was studied in detail, it was apparent from initial photochemical investigations of complexes **2**, **3**, and **4** that the nature of the arene has a significant effect on the course of the reaction. As for complex **1**, complex **2** containing benzene as the arene underwent arene loss upon irradiation (Figures S3 and S4), but complexes **3** and **4** containing *p*-cymene and hexamethylbenzene, respectively, as arenes did not readily undergo arene loss (see Supporting Information). Hence it appears that complexes containing arenes which are the strongest donors (e.g., hexamethylbenzene) are the most stable to light.

DNA Binding. The samples of DNA and **1** were prepared in three ways: in the dark (henceforth referred to as non-irradiated), following the addition of pre-irradiated **1** to DNA (pre-irradiated), or by addition of **1** to DNA followed by irradiation of the resulting mixture (irradiated). The samples were irradiated by light with peak intensity at 360 nm for 60 min. Solutions of CT DNA at a concentration of 50 μg mL^{-1} were incubated with **1** at an r_i value of 0.1 in 10 mM $NaClO_4$ or 0.1 M NaCl at 310 K (r_i is defined as the molar ratio of free ruthenium complex to nucleotide-phosphates at the onset of incubation with DNA). At various time intervals, an aliquot of the reaction mixture was withdrawn, quickly cooled in an ice bath, and precipitated by ethanol and the content of ruthenium in the supernatant of these samples was determined by FAAS. The number of atoms of ruthenium bound per nucleotide residue, r_b, was calculated by subtraction of the amount of free (unbound) ruthenium from the total amount of ruthenium present in the reaction. The binding of the ruthenium compounds to CT DNA was also quantified in two other ways. The samples containing the reaction mixture were quickly cooled on an ice bath and then exhaustively dialyzed against 10 mM $NaClO_4$ at 277 K or filtered using Sephadex G50 to remove free (unbound) ruthenium. The content of ruthenium in these DNA samples was determined by FAAS. The values of r_b obtained using this assay were identical to those based on DNA precipitation by ethanol.

The binding experiments (summarized in Table 2) indicate that the non-irradiated, pre-irradiated, and irradiated forms of **1** reacted with DNA readily in 10 mM $NaClO_4$ (95, 100, and 100%, respectively, reacted after 20 h), while the presence of the 0.1 M NaCl reduced the amount bound to DNA, particularly in the case of the reactions of the non-irradiated **1**. The binding of non-irradiated, pre-irradiated, or irradiated **1** to DNA was almost complete after 20 h, although that of non-irradiated **1** was slower (Table 2). Importantly, the analytical method used monitors the relatively strong binding of the ruthenium complex to DNA (so that the results are not affected by eventual subsequent closure of monofunctional adducts to cross-links). No pH

Table 2. Binding of Non-Irradiated, Pre-irradiated, or Irradiated **1** to Calf Thymus DNA in 10 mM $NaClO_4$ or 0.1 M NaCl as Determined by FAAS

	non-irradiated **1**[a]		pre-irradiated **1**[a,b]		irradiated **1**[a,c]	
medium	B_{20h} (%)[d]	$t_{50\%}$ (h)[e]	B_{20h} (%)[d]	$t_{50\%}$ (h)[e]	B_{20h} (%)[d]	$t_{50\%}$ (h)[e]
10 mM $NaClO_4$	95	5.4	100	1.1	100	2.6
0.1 M NaCl	<10	NA[f]	70	ND[g]	70	ND[g]

[a] Incubations with DNA were at 310 K. The concentration of DNA was 50 μg mL^{-1}, and r_i was 0.1. Data are the average of three independent experiments. [b] Irradiation of **1** was carried out in absence of DNA for 60 min, followed by a further incubation with DNA in the dark. [c] Irradiation of **1** was carried out in presence of DNA for 60 min, followed by a further incubation in the dark. [d] Amount of bound ruthenium after 20 h. [e] The incubation time needed to reach 50% binding. [f] Not applicable. [g] Not determined.

changes were observed for reaction mixtures containing DNA and non-irradiated, pre-irradiated, or irradiated **1** within 20 h after mixing DNA with the ruthenium complex. Because of the relatively very low binding rate for the non-irradiated form of **1** in 0.1 M NaCl, further experiments with DNA were performed with non-irradiated or pre-irradiated forms of **1** in 10 mM $NaClO_4$ or **1** was irradiated in the presence of DNA in 10 mM $NaClO_4$ for 60 min and further incubated in the dark for additional 24 h; experiments in which DNA was modified in 0.1 M NaCl were performed only with pre-irradiated **1**.

In Vitro Transcription of DNA Containing Adducts of 1. In vitro RNA synthesis by RNA polymerases on DNA templates containing several types of bifunctional adducts of platinum or ruthenium complexes can be prematurely terminated at the level or in the proximity of DNA adducts. Importantly, monofunctional DNA adducts of several platinum complexes are unable to terminate RNA synthesis.[25]

Cutting of pSP73KB DNA by *Nde*I and *Hpa*I restriction endonucleases yielded a 212-bp fragment (a substantial part of its nucleotide sequence is shown in Figure 7b).[25] This fragment contained a T7 RNA polymerase promotor [close to the 3′-end of the top strand (Figure 7b)]. The experiments were carried out using this linear DNA fragment, modified at $r_b = 0.005$ by both non-irradiated (with and without subsequent irradiation at 360 nm) and pre-irradiated forms of **1** in 10 mM $NaClO_4$ or by pre-irradiated **1** in 0.1 M NaCl, for RNA synthesis by T7 RNA polymerase (Figure 7a, lanes 1−5). In addition, **1** was irradiated for 60 min in the presence of the unmodified fragment (in 10 mM $NaClO_4$) and subsequently incubated in the dark for an additional 20 h (Figure 7a, lane 6).

RNA synthesis on the fragment modified by non-irradiated, pre-irradiated, and irradiated forms of **1** yielded fragments of newly synthesized RNA of defined sizes, which indicates that RNA synthesis on these templates was prematurely terminated. The major stop sites produced by all samples of ruthenated DNA fragments occurred at similar positions in the gel and were mainly at guanine residues. Interestingly, the total intensity of the bands on the autoradiogram corresponding to transcripts of single-ruthenated DNA fragments [modified to the same level (r_b)] differed.

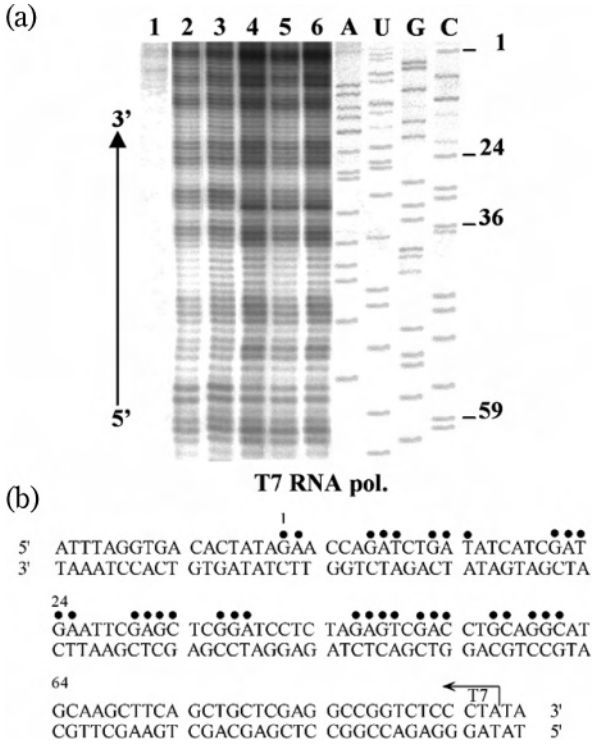

Figure 7. Inhibition of RNA synthesis by T7 RNA polymerase on the *Nde*I/*Hpa*I fragment of the pSP73KB plasmid modified by **1**. This linear DNA fragment was modified for 20 h by non-irradiated **1** (with or without subsequent irradiation for 60 min at 360 nm, lanes 2 and 3 in Figure 7a), pre-irradiated **1** in 10 mM $NaClO_4$ (lane 4), pre-irradiated **1** in 0.1 M NaCl (lane 5), or the unmodified fragment was mixed with non-irradiated **1** in 10 mM $NaClO_4$ and the mixture was irradiated for 60 min and subsequently incubated in the dark for additional 20 h (lane 6 in Figure 7a) so that the resulting r_b value was 0.005. (a) Autoradiogram of 6% polyacrylamide/8 M urea sequencing gel. Lanes: (1) control, nonmodified template; (2) the template modified by non-irradiated **1**; (3) the same as in lane 2, but the sample was subsequently irradiated; (4 and 5) the template modified by pre-irradiated **1** in 10 mM $NaClO_4$ or 0.1 M NaCl, respectively; (6) the template was mixed with non-irradiated **1** in 10 mM $NaClO_4$ and the mixture was irradiated for 60 min and subsequently incubated in the dark for additional 20 h; (A, U, G, C) chain-terminated marker RNAs. For the details, see the text. (b) Schematic diagram showing the portion of the nucleotide sequence of the template of the *Nde*I/*Hpa*I fragment used to monitor inhibition of RNA synthesis. The arrow indicates the start of the T7 RNA polymerase and ● indicates the major stop signals (from Figure 7a, lane 3). The numbers correspond to the nucleotide numbering in the sequence map of pSP73KB plasmid.

The bands corresponding to the transcription of DNA modified by the non-irradiated **1** were faint (Figure 7a, lane 2); the intensity of those corresponding to the transcription of DNA modified by the non-irradiated **1** that was subsequently irradiated was moderate (Figure 7a, lane 3), and the intensity of those corresponding to the transcription of DNA modified by pre-irradiated **1** or if the unmodified fragment was irradiated together with **1** (and subsequently incubated in the dark for additional 20 h) were strongest (Figure 7a, lanes 4 and 6, respectively). In addition, the bands produced by the transcripts of DNA fragments modified by pre-irradiated **1** in the presence of 0.1 M NaCl were weaker (Figure 7a, lane 5) in comparison with those modified in 10 mM $NaClO_4$. Taken together, the results of the transcription mapping experiments (Figure 7) suggest that the non-irradiated form of **1** preferentially forms DNA adducts that represent only a weak block for RNA polymerase, presumably monofunctional adducts. The subsequent irradiation of

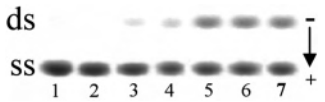

Figure 8. Formation of the interstrand cross-links by **1** in pSP73KB plasmid (2455bp) linearized by *Eco*RI. DNA was incubated with the complex for 20 h so that the r_b value was 0.001. Autoradiograms of denaturing 1% agarose gels of linearized DNA which was 3′-end labeled. The interstrand cross-linked DNA appears as the top bands migrating on the gel more slowly than the single-stranded DNA (contained in the bottom bands). Lanes: (1 and 2) control, nonmodified DNA in 10 mM $NaClO_4$ and 0.1 M NaCl, respectively; (3) DNA modified by non-irradiated **1** in 10 mM $NaClO_4$; (4) the same as in lane 3, but the sample was subsequently irradiated; (5 and 6) DNA modified by pre-irradiated **1** in 10 mM $NaClO_4$ and 0.1 M NaCl, respectively; (7) DNA was mixed with non-irradiated **1** in 10 mM $NaClO_4$ and the mixture was irradiated for 60 min and subsequently incubated in the dark for additional 20 h.

DNA already modified by the non-irradiated **1** transforms the adducts so that they become stronger blocks for RNA polymerase, presumably to some type of cross-links. The modification of DNA by the pre-irradiated form of **1** results in adducts which efficiently terminate RNA synthesis so that it is reasonable to suggest that pre-irradiated **1** preferentially forms cross-links. In addition, the results of transcription mapping indicate that the presence of chloride in the medium in which DNA was modified somewhat lowers the propensity of the pre-irradiated form of **1** to form bifunctional adducts, implying that the Ru−Cl bonds are less reactive than Ru−OH_2 bonds in **1**.

DNA Interstrand Cross-linking. Bifunctional platinum- or ruthenium-based drugs form both intrastrand and interstrand cross-links on DNA. Although some of these compounds (for instance cisplatin) form interstrand cross-links on DNA with only a low frequency, these lesions are also considered relevant to the antitumor effects of metal-based drugs.[17] The amounts of interstrand CLs formed by both non-irradiated and pre-irradiated forms of **1** in the presence or absence of DNA in pSP73KB plasmid linearized by *Eco*RI (which cuts this plasmid only once) were determined. The experiments were carried out using this linear DNA fragment, modified at $r_b = 0.001$ by non-irradiated **1** in 10 mM $NaClO_4$ or by pre-irradiated **1** in 0.1 M NaCl. The fragment modified by non-irradiated **1** was divided into two parts, and one was subsequently irradiated for 60 min by light with peak intensity at 360 nm. The samples were analyzed for interstrand CLs by agarose gel electrophoresis under denaturing conditions.[25−27] The very faint bands corresponding to more slowly migrating interstrand-cross-linked fragments were observed (Figure 8). The radioactivity associated with the individual bands in each lane was measured to obtain estimates of the fraction of non-cross-linked or cross-linked DNA under each condition. The frequencies of interstrand CLs produced by **1** under different conditions are shown in Table 3.

The efficiency of pre-irradiated **1** to form DNA interstrand cross-links in both 10 mM $NaClO_4$ and 0.1 M NaCl under the conditions described in the experimental section is slightly higher than that of cisplatin. In contrast, the interstrand crosslinking efficiency of non-irradiated **1** in 10 mM $NaClO_4$ is relatively low. Somewhat enhanced amounts of interstrand cross-links were observed if the sample of

Table 3. DNA Interstrand Cross-Linking of Linearized pSP73KB Plasmid by **1**[a]

medium	non-irradiated **1**[b]	irradiated after incubation with DNA[c]	pre-irradiated **1**[d]	irradiated **1**[e]
10 mM $NaClO_4$	2%	4%	7%	7%
0.1 M NaCl	ND[f]	ND[f]	7%	ND[f]

[a] The r_b was 0.001. Data are the average of three independent experiments. [b] The linearized plasmid was incubated with non-irradiated **1** for 20 h. [c] The linearized plasmid was incubated with non-irradiated **1** in the dark for 20 h, and then it was irradiated for 60 min with light of maximum intensity at 360 nm [in the absence of free (unbound) ruthenium complex]. [d] An aqueous solution of **1** was pre-irradiated for 60 min (in the absence of DNA) and then added to the linearized plasmid and incubated for 20 h. [e] Irradiation of **1** was carried out in presence of DNA for 60 min, followed by a further incubation in the dark. [f] Not determined.

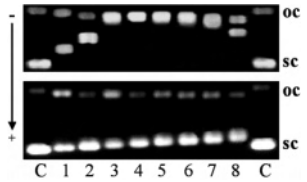

Figure 9. Unwinding of supercoiled pSP73KB plasmid DNA modified by pre-irradiated **1** in 10 mM $NaClO_4$ (top panel) or 0.1 M NaCl (bottom panel). Lanes: (C) control, unmodified DNA; (1−8) r_b = 0.040, 0.060, 0.075, 0.085, 0.095, 0.11, 0.12, and 0.14, respectively. The top bands correspond to the form of nicked plasmid (oc) and the bottom bands to closed negatively supercoiled plasmid (sc).

DNA already modified by non-irradiated **1** [in absence of free (unbound) ruthenium complex] was then irradiated. This observation is consistent with the idea that the subsequent irradiation of DNA already modified by non-irradiated **1** transforms some adducts into interstrand cross-links. In addition, the results on interstrand cross-linking indicate that the presence of chloride in the medium in which DNA was modified does not lower the propensity of pre-irradiated **1** to form interstrand cross-links.

DNA Unwinding. Electrophoresis of native agarose gels can be used to determine the unwinding induced in negatively supercoiled pSP73 plasmid by monitoring the degree of supercoiling (Figure 9).[28] A compound that unwinds the DNA duplex reduces the number of supercoils in closed circular DNA. This decrease upon binding of unwinding agents causes a decrease in the rate of migration through agarose gel, which makes it possible to observe and quantify the mean value of unwinding per adduct.

Variable amounts of **1** (pre-irradiated, irradiated in the presence of DNA, or non-irradiated forms in 10 mM $NaClO_4$ and the pre-irradiated form in 0.1 M NaCl) were bound to a mixture of relaxed and negatively supercoiled pSP73 DNA. The resulting products were analyzed by gel electrophoresis (shown in Figure 9 for the modification by pre-irradiated **1** in 10 mM $NaClO_4$ in the top panel and in 0.1 M NaCl in the bottom panel). The mean unwinding angle is given by $\Phi = 18\sigma/r_b(c)$, where σ is the superhelical density and $r_b(c)$ is the value of r_b at which the supercoiled and nicked forms comigrate.[28] Under the present experimental conditions, σ was calculated to be −0.063 using the data for cisplatin, for which the $r_b(c)$ was determined in this study and $\Phi = 13°$ was assumed. The DNA unwinding angle produced by the adducts formed by non-irradiated, pre-irradiated, and irradi-

ated forms of **1** in 10 mM $NaClO_4$ was determined to be 13 ± 2°, using this approach. In contrast, no comigration of the supercoiled and nicked forms was reached from modification of DNA by pre-irradiated **1** in 0.1 M NaCl even at an r_b value as high as 0.14 (Figure 9, bottom panel) so that the adducts formed by pre-irradiated **1** unwound DNA only negligibly (<3°). Thus, the adducts of **1** formed on DNA in 10 mM $NaClO_4$ share a common conformational feature responsible for a relatively high level of DNA unwinding. On the other hand, the conformation of DNA adducts formed by the pre-irradiated form of **1** in 0.1 M NaCl is apparently considerably different and does not induce DNA unwinding.

Conclusions

We have shown that the dinuclear Ru^{II} arene complex [{-(η^6-indan)RuCl}$_2$(μ-2,3-dpp)]$(PF_6)_2$ (**1**) can undergo hydrolysis in aqueous solution in the dark. Ru−OH_2 bonds are more reactive than Ru−Cl bonds, and the aqua adducts can bind to DNA and, to a small extent, can form interstrand cross-links on plasmid DNA. The transcription mapping experiments suggest that guanines might be preferential binding sites. Subsequent irradiation of the ruthenated DNA or irradiation of **1** in the presence of DNA led to an increased frequency of cross-linking. This was explained on the basis of the increased reactivity of ruthenium caused by arene loss upon irradiation. Photoinduced arene loss from the complex, in the absence of DNA, was readily monitored by its increased fluorescence intensity (∼40×) when unbound compared to bound. Indan release was confirmed by time-resolved fluorescence and NMR spectroscopy. Mononuclear Ru^{II} arene complexes [(η^6-arene)Ru(N,N)Cl]$^+$, including indan derivatives, where (N,N) is a chelating diamine ligand, can exhibit anticancer activity and are usually stable in the light. The dinuclear indan complex studied here is a member of a new family of potential anticancer complexes for which it might be possible to enhance activity by photoactivation. Although the benzene analog (**2**) can also undergo photoinduced arene loss, complexes with more strongly bound arenes (e.g., hexamethylbenzene) do not. Photoactivation of metal complexes may have the advantage of producing novel types of DNA cross-links that cannot be readily achieved by chemical reactions alone. These novel lesions may avoid repair mechanisms and lack cross-resistance with other classes of anticancer agents. The detection of fluorescence from the released arene offers the possibility of monitoring the course of such cytotoxic reactions inside tissues or, even, individual cells.

Acknowledgment. This research was supported by the Scottish Higher Education Funding Council (COSMIC), the Grant Agency of the Czech Republic (Grants 305/05/2030 and 203/06/1239), and the Academy of Sciences of the Czech Republic (Grants 1QS500040581 and KAN200200651). The authors also acknowledge that their participation in the EU COST Action D20 enabled them to exchange ideas with European colleagues.

Supporting Information Available: UV−vis spectra for photoproducts of **1** in water and 0.1 M NaCl and UV-vis and fluorescence spectra in methanol (Figures S1 and S2), syntheses and irradiation experiments for complexes **2**, **3**, and **4**, UV−vis and NMR spectra for irradiation of **2** (Figures S3 and S4), and X-ray crystallographic data for **1** in CIF format. This material is available free of charge via the Internet at http://pubs.acs.org.

IC062111Q